Synthesis, mesomorphic behaviour and luminescence of a polymerisable perylene-tetra(carboxylate-hexene) liquid crystal

Guang Hu[1*], Xinyang Wu[1], Yumin Tang[2], Wei Qian[1], Weiwei Hu[1], Huanjun Lu[3*], Liang Song[1], Kailong Zhang[1], Xiangbing Zeng[2*]

[1] Key Laboratory for Palygorskite Science and Applied Technology of Jiangsu Province, Faculty of Chemical Engineering, Huaiyin Institute of Technology, Huaian, 223003, China.
[2] School of Chemical, Materials Science and Biological Engineering, University of Sheffield, Sheffield, S1 3JD, UK.
[3] Key Laboratory of Intelligent Optoelectronic Devices and Chips of Jiangsu Higher Education Institutions, School of Physical Science and Technology, Suzhou University of Science and Technology, Suzhou, 215009, China.

Corresponding Authors:
Dr. Guang Hu.
Key Laboratory for Palygorskite Science and Applied Technology of Jiangsu Province, Faculty of Chemical Engineering, Huaiyin Institute of Technology, Huaian, 223003, China.
Email: guanghu2019@hyit.edu.cn;

Dr. Huanjun Lu.
Key Laboratory of Intelligent Optoelectronic Devices and Chips of Jiangsu Higher Education Institutions, School of Physical Science and Technology, Suzhou University of Science and Technology, Suzhou, 215009, China.
Email: luhuanjun@usts.edu.cn

Dr. Xiangbing Zeng
School of Chemical, Materials Science and Biological Engineering, University of Sheffield, Sheffield, S1 3JD, UK.
Email: x.zeng@sheffield.ac.uk

Abstract
A polymerisable perylene-tetra(carboxylate-hexene) liquid crystal was synthesised to study their mesomorphic behaviour and transition temperatures using polarised optical microscopy (POM), differential scanning calorimetry (DSC) and small/wide angle X-ray scattering (S/WAXS). The optimised 3D geometry model using TD-DFT Gaussian theoretical calculation was presented to build the relationship between mesophases and molecular configuration. The UV-Vis absorption and fluorescent emission have also been measured to evaluate their potentials for use as promising liquid crystalline organic semiconductors. The results demonstrate a favourable room-temperature liquid crystal with wide range of mesophase and good luminescent properties.

Keywords
Perylene derivatives; room-temperature liquid crystals; wide mesophases; polymerisable liquid crystals

1. Introduction

Highly conjugated, fused, aromatic perylene derivatives have been widely reported for use as organic semiconductors in opto-electronic devices, such as organic light-emitting diodes(OLEDs), organic photovoltaics (OPVs) and organic field-effect transistors (OFETs) due to their high luminescence, chemical and thermal stability, low cost and ease of functionalization[1-6]. Among these derivatives, perylene-based liquid crystalline organic semiconductors have attracted much attention due to their unique mesophases with ordered molecular packing and self-assembling which are favourable for high charge mobility and luminescent properties[7-10]. The perylene-based derivative structures with planar, disc-shaped aromatic cores and several flexible chains possess a large advantage to construct liquid crystalline materials which exhibit fast charge transporting ability due to strong π-π interactions and stacking of disk aromatic cores[11-15].

Liquid crystalline organic semiconductors have been developed for many years and they exhibit high charge transporting ability and electroluminescent properties with low threshold voltage and high quantum efficiency and light outcoupling in the opto-electronic devices due to the presence of ordered liquid crystalline mesophases which lead to the fabrication of high-quality thin films with macroscopically homogeneous molecular alignment and the absence of crystal boundary defects to the quenching of holes/electrons[16]. However, the appropriate mesophase transition temperatures and wide ranges of liquid crystalline phases are required for successfully exploiting these advantages to manufacture highly efficient thin-film devices. The room-temperature liquid crystalline materials[17-20] are always favourable for practical application because various opto-electronic appliances such as flat-panel TV displays, notebooks, digital cameras, and domestic devices work in the room temperature, and wide mesophases also afford a large temperature range in fabricating these devices.

Although perylene-based materials have been reported as organic semiconductors, less attention was paid to the detailed investigation of their liquid crystalline behaviour and the identification of room-temperature and wide mesophases for perylene-based liquid crystals. Therefore, in this work, we designed and synthesised a novel perylene-tetra(carboxylate-hexene) room-temperature liquid crystal with wide mesophase range of about 180°C. Its mesomorphic behaviour and transition temperatures were clearly studied by using polarised optical microscopy (POM), differential scanning calorimetry (DSC) and small/wide angle X-ray scattering (S/WAXS). The optimised 3D geometry model using TD-DFT Gaussian theoretical calculation was presented to build the relationship between mesophases and molecular configuration. The UV-Vis absorption and fluorescent emission have also been measured to evaluate their potentials for use as promising liquid crystalline organic semiconductors. In addition, flexible alkene chains were also designed to achieve the polymerisable properties which are required for low-cost solution-processed organic semiconductors due to the combined advantages of flexible fabrication, solubility, purity and batch-to-batch repeatability[21-26]. Furthermore, Polymerisable liquid crystalline materials also create many new applications, such as photo-curing 3D/4D printing[26-31]. Therefore, we believe the study of mesomorphic behaviour and luminescent properties for polymerisable perylene-based room-temperature liquid crystals would promote the fast development of organic semiconductors and some new applications.

2. Experimental

2.1. Materials and methods

All commercially available starting materials and reaction intermediates, reagents and solvents were obtained from Bide Pharma, Energy Chemical and Aladdin, and were used as provided unless otherwise stated. The ^{1}H and ^{13}C NMR spectra were recorded using Bruker AVANCE NEO spectrometer. High Resolution Mass spectra (HRMS) were recorded using Agilent 6545 Q-TOF electrospray ionization mass spectrometer (ESI-MS). The melting point and transition temperatures for the liquid crystal compound were measured using polarizing optical microscopy (POM), with an England Linkam THMS600 hot/cold platform and an Germany Leica DM2500 polarizing microscope. The powder of sample about 0.05 mg was placed between two glass slides with slight pressure to prepare a thin film for POM measurement with heating/cooling cycles at 5°C/min. The thermal analysis was measured by using differential scanning calorimetry (DSC) with the Netzsch DSC 214, and the heating rate and cooling rate were both 10°C/min. Small/wide angle X-ray scattering (S/WAXS) experiments were carried out on an X-ray scattering instrument (SAXSess mc^2, Anton Paar) equipped with line collimation and a 2200 W sealed-tube X-ray generator (Cu-Kα, λ = 0.154 nm). Powder samples about 3 mg were wrapped in aluminum foil for S/WAXS experiments with heating/cooling cycles at 10 °C/min. The sample was kept under vacuum during irradiation. An imaging plate was used to record the scattering pattern. Silver behenate was used as the calibration standard. The

UV-Visible absorbance spectra were measured using a Japan Shimadzu UV-2401 type UV spectrophotometer and the sample was dissolved in dichloromethane with a concentration of 33 mg/L. The Hitachi F-7000 fluorescence spectrophotometer was used to measure the fluorescence of the material with a concentration of 3.3 mg/L in dichloromethane.

2.2. Material synthesis

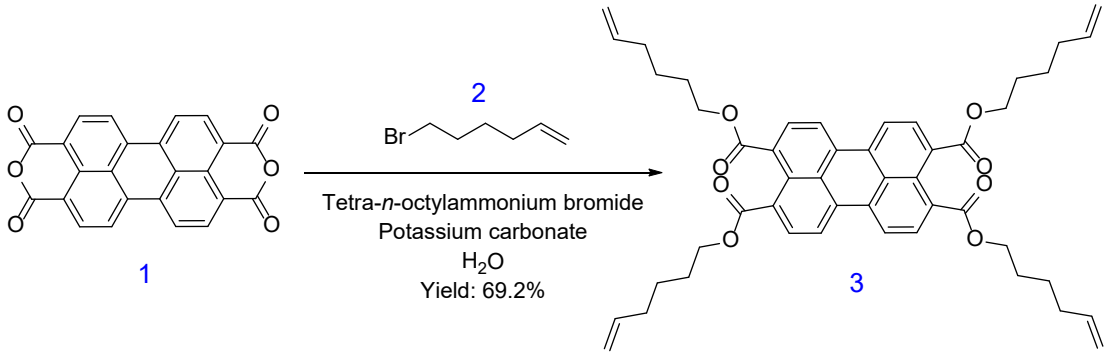

Scheme 1. The reaction pathway used to synthesize the perylene-based compound 3

Ttetra(hex-5-en-1-yl) perylene-3,4,9,10-tetracarboxylate (compound 3)

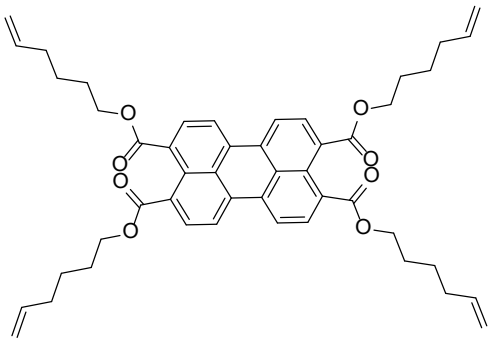

3,4,9,10-tetracarboxylic anhydride (0.5 g, 1.28 mmol), K_2CO_3 (2.5 g, 18 mmol), TOAB tetraoctylammonium bromide (0.2734 g, 0.5 mmol), and 6-bromo-1-hexene (13.5 cm^3, 51.5 mmol) were dissolved in water by adding a stirrer to a dry, 250 mL round bottomed beaker (100 ml). Subsequently, the reaction was refluxed with stirring in an oil bath for over 3 days. Subsequently cooled to room temperature was extracted with dichloromethane (5×100 cm^3), the organic layer was collected, washed with saturated brine, dried over anhydrous sodium sulfate and the solvent was removed by distillation under reduced pressure to obtain the crude product. The crude product was purified by silica gel column chromatography using petroleum ether/dichloromethane (3:1) as eluent, and finally the product was further purified by silica gel plate using petroleum ether/dichloromethane (1:1-1:2) as unfolding agent to give the desired product as an orange-yellow solid (0.67 g, 69.2%). The reaction pathway used to synthesize compound 3 was shown in Scheme 1.

^{1}H NMR (600 MHz, $CDCl_3$) δ 8.19 (d, *J* = 8.0 Hz, 4H), 7.98 (d, *J* = 7.9 Hz, 4H), 5.83 (ddt, *J* = 16.9, 10.2, 6.7 Hz, 4H), 5.05 (dd, *J* = 17.1, 1.6 Hz, 4H), 5.01-4.96 (m, 4H), 4.34 (t, *J* = 6.8 Hz, 8H), 2.15 (q, *J* = 7.2 Hz, 8H), 1.82 (dt, *J* = 14.8, 6.9 Hz, 8H), 1.61-1.53 (m, 8H).

^{13}C NMR ($CDCl_3$) δ 168.63, 138.42, 132.81, 130.30, 128.72, 121.36, 115.07, 65.48, 33.47, 28.16, 25.39.

HRMS(ESI) calcd for $C_{48}H_{52}O_8$ (M^+Na): 779.3559, found: 779.3579.

3. Results and discussion

3.1. Synthetic discussion

The compound 3 was synthesized by using simple one-step route with medium yield 69.2% according to modified literature methods[32-33]. The one-step reaction to produce polymerizable liquid crystalline materials is preferred because fewer reaction steps are beneficial for mass production, especially for some new applications requiring large amount of materials, such as 3D printing liquid crystal elastomers. The reaction of anhydride and alkyl bromide belongs to a nucleophilic substitution. After a ring-opening reaction of anhydride, the carboxyl group is hydrolyzed to produce carboxyl anion which is nucleophilic-substituted with carbon-bromine. The excessive alkyl bromide is for the purpose of achieving a complete substitution of four alkene chains and reduces by-products, which could be beneficial for a good yield near to 70%. However, a high temperature at 110°C and long reaction time over 3 days for avoiding the incomplete alkyl-substituted by-products in the heterogenous reaction with a large diffusion resistance could lead to a decrease of the yield and the low boiling point of alkyl bromide may also generate more by-products, thus further decreasing the yield.

3.2 Mesomorphic behaviour, phase transition temperatures and photo-physical properties

Polarized light microscopy (POM) was firstly used to observe liquid crystalline phases and transition temperatures of compound 3 upon heating and cooling cycles. Figure 1(a-d) gives the POM images of compound 3 cooling at different temperatures with 195°C, 160°C, 97°C and 10°C, respectively. When the sample of compound 3 was heated up to 200°C, it completely melted into isotropic state with a full black background. Then the irregular, broken, fan-like texture began to appear when the sample was cooled to 195°C, as shown in Figure 1(a). As the temperature continued to decrease, the texture became larger and overlapped to grow, presenting more colourful, polygonal, textures, as shown in Figure 1(b-c) cooling to 160°C and 97°C, respectively. The images looks like a pseudo focal conic fan-shaped texture which could be assigned to either a columnar or lamellar phase. The mesophase was retained with the decrease of temperature until when the sample was cooled to 10°C, crystalline texture began to appear and cover the fan-shaped texture, as shown in Figure 1(d).

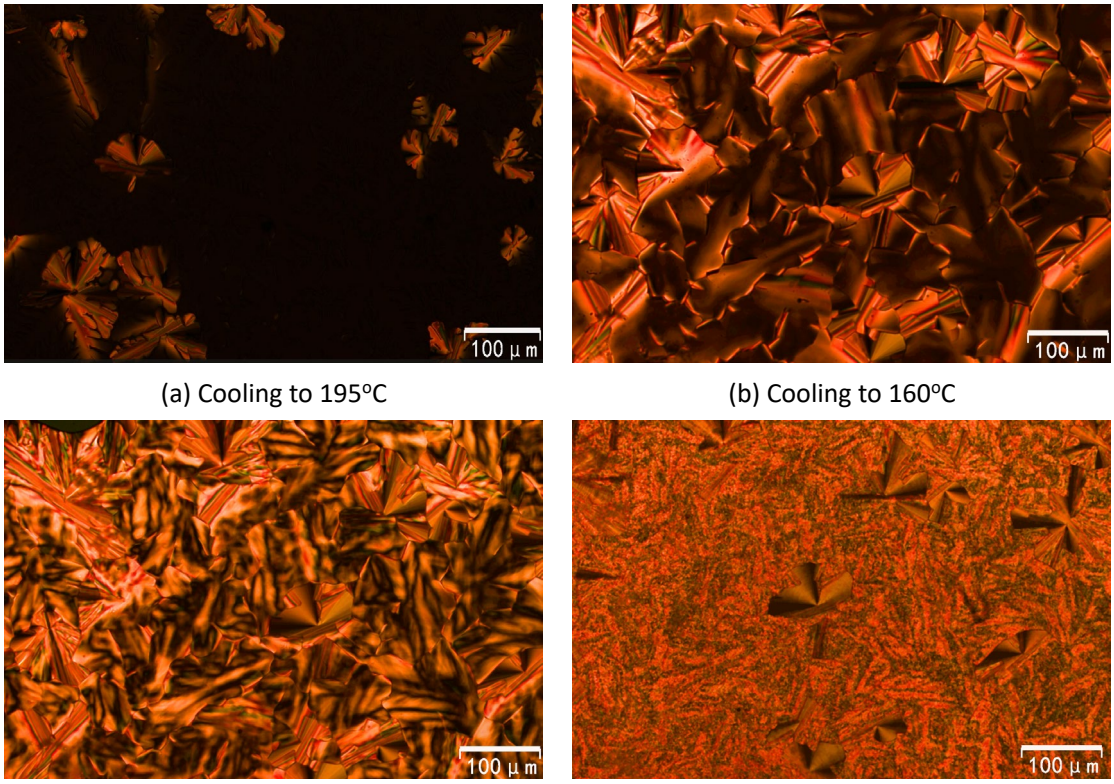

(a) Cooling to 195°C (b) Cooling to 160°C

(c) Cooling to 97°C (d) Cooling to 10°C

Figure 1. The POM images observed for compound 3 on cooling at 195°C (a), 160°C (b), 97°C (c) and crystalline texture at 10°C (d).

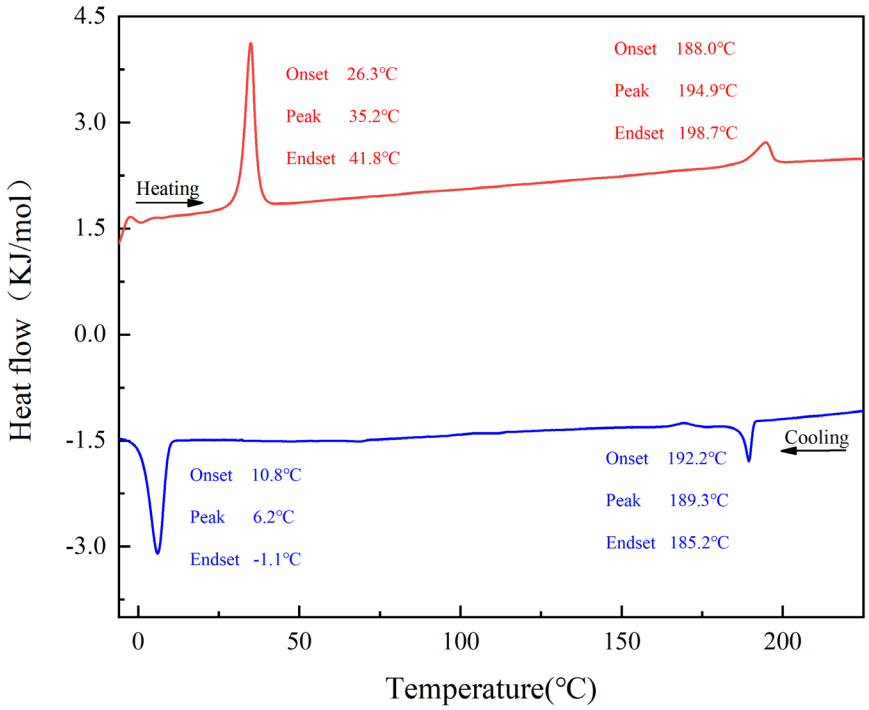

Figure 2. The heating and cooling cycle of the DSC trace as a function of temperature for compound 3 (scan rate 10°C/min)

The DSC analysis was also use to confirm mesophase transition temperatures for compound 3, and the curve was shown in Figure 2. We can see clearly from the heating curve that the compound 3 completely melted into isotropic state at approximately 199°C which is consistent with the clearing point observed from POM. During the cooling process, a typical small peak from isotropic state to liquid crystalline phase appeared at about 192°C which is basically consistent with the characteristic temperature (195°C) observed from POM. However, the big crystallization peak from liquid crystalline phase to crystalline appeared lately until the temperature cooled to approximately 11°C, which is also consistent with the appearance of crystalline texture upon cooling at 10°C observed from POM. The small deviation of the transition temperatures measured by different analytical equipment, such as POM, DSC or XRD, is common due to kinetic effects that can be affected by heating and cooling rates, sample thickness and position, and measurement method. The results overall confirm a room-temperature, wide range of mesophase for the liquid crystalline compound 3.

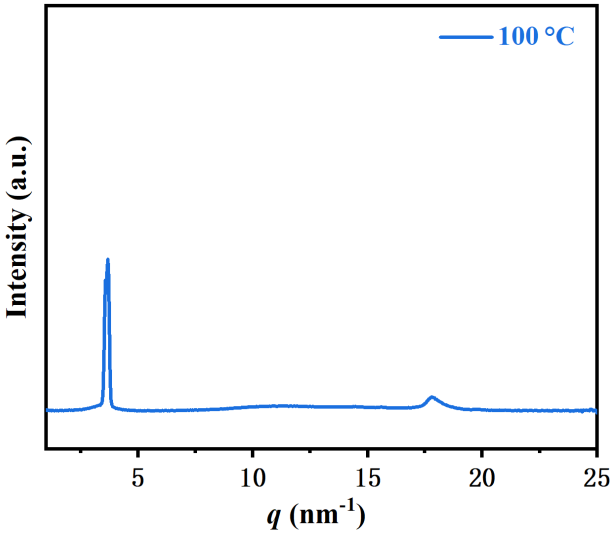

Figure 3. SAXS/WAXS patterns of compound 3 at 100 °C on heating.

The Small- and Wide-Angle X-Ray Scattering (SAXS/WAXS) measurement was used to further confirm the mesophase of compound 3. In the low-angle region, the SAXS pattern (Figure 3) revealed a single, sharp reflection at q = 3.64 nm^{-1}, corresponding to a d-spacing of 1.73 nm. This d-spacing is clearly smaller than the extended length of the molecule, and instead roughly equals to the length of the aromatic core (~0.8 nm) plus one of the flexible alkyl chains (~1.1 nm). Assuming a smectic structure, the slightly smaller measured value of 1.73 nm can be reasonably attributed to conformational disorder and partial coiling of the molten alkyl chains in a conventional monolayer smectic phase. The molecule could be arranged in layers with their aromatic cores roughly parallel and their flexible chains extending on both sides, interdigitating and mixing with the chains from the adjacent layers. This interpretation is further supported by the broad wide-angle halo at q = 17.8 nm^{-1} (d = 0.35 nm), which confirms the π-π stacking of the aromatic cores.

The fact that there are no high order diffraction peaks observed for the mesophase suggest a high thermal motion in the mesophase, hence a high Debye-Waller factor that suppresses the diffraction intensities of high order diffractions. Consequently, we believe it should possess a lamellar packing instead of a discotic columnar one, as the 1D structure of the former would allow a larger amount of thermal motion compared to the 2D structure of the columnar phase.

This smectic structure formed from discotic molecules may be caused by the decreased length of the end alkyl chain[34-35]. Support to this argument is provided by our studies on its homologue with longer octene chains[36]. As confirmed by SAXS (Figure 4a), the longer octene-chain analogue (Figure 4b) clearly exhibits a well-defined hexagonal columnar (Col_h) phase, the archetypal structure for discotic liquid crystals. Unlike in compound 3, high order diffraction orders up to (210) of the columnar phase is clearly observed. We believe that the longer, more voluminous octene chains could effectively act as a solvent-like aliphatic mantle, promoting a high degree of core-chain segregation. This drives the molecules to stack into columns, which then pack into a 2D hexagonal lattice for optimal efficiency. The electron density map of the Col_h phase formed in the analogous reference compound with four longer octene chains has also been clearly shown in Figure 5.

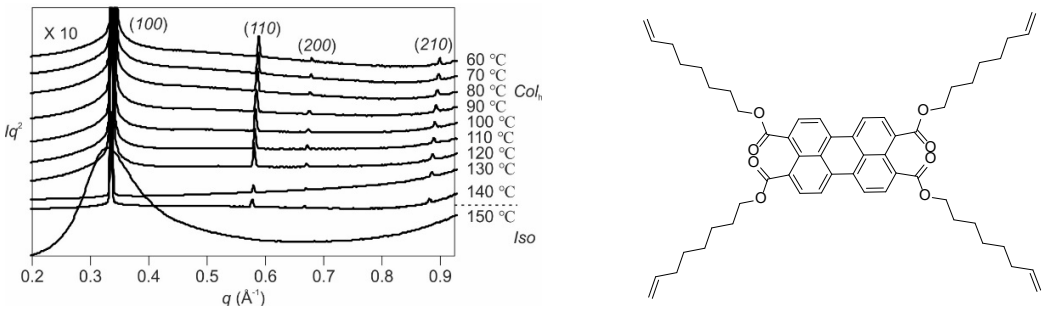

(a) (b)

Figure 4. SAXS patterns on cooling from 150 to 60 °C (a) and the chemical structure (b) of the analogous reference compound with four longer octene chains.

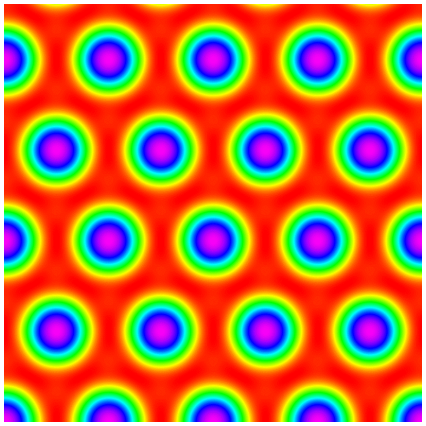

Figure 5. Electron density map of the Col_h phase formed in the analogous reference compound with four longer octene chains.

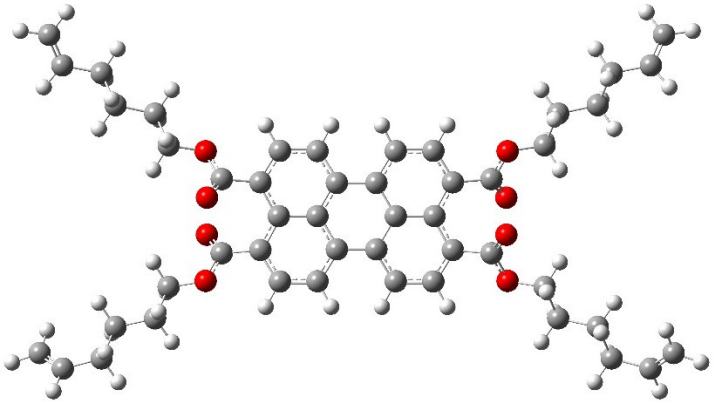

Figure 6. The optimised 3D geometry model of compound 3 by TD-DFT calculation using Gaussian 16 at the B3PW91/6–31G(d) level.

The optimised 3D geometry model of compound 3 was obtained by TD-DFT calculation using Gaussian 16 at the B3PW91/6–31G(d) level, as shown in Figure 6. While the perylene core is perfectly suited for columnar formation, the shortened hexene chains could be responsible for the presence of discotic lamellar structure via altering the intermolecular forces and packing constraints. The aromatic cores segregate into sub-layers, each of which can be viewed as adopting a nematic-like structure, where the disc-like cores still maintain their π-π interactions (as evidenced by the broad WAXS peak at approximately 0.35 nm). The shorter hexene chains interdigitate (mix and intertwine) with each other in the adjacent aliphatic sub-layers, filling space efficiently and creating a one-dimensional periodicity of the layers. High mobility of the molecules is expected in such a structure, and could be the origin of the single, sharp SAXS peak observed corresponding to the layer thickness (~1.73 nm). The optimised TD-DFT geometry model (Figure 6) confirms the classic disc-shaped structure of compound 3. However, this model only shows the shape of a single molecule. The key to understanding its mesophase lies in predicting how hundreds of these molecules will pack together. The flexible alkyl chains, while not altering the intrinsic disc-like shape of the single molecule, alter the collective packing of the ensemble.

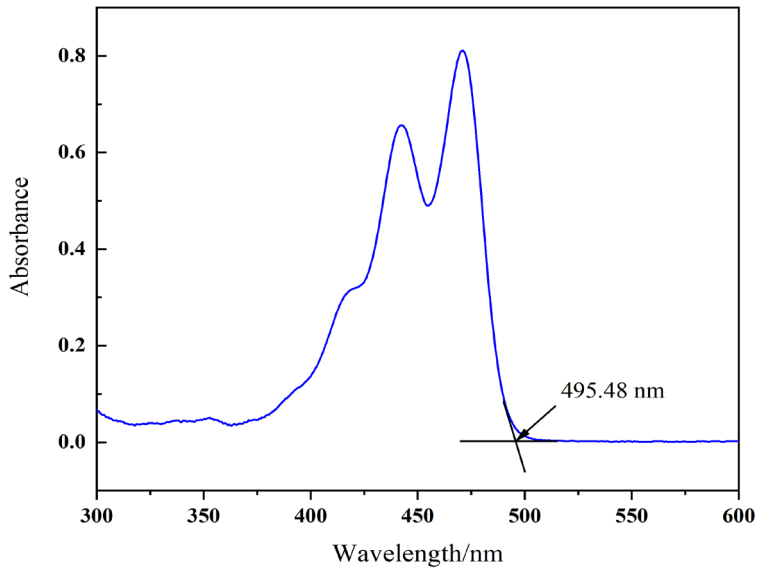

Figure 7. The UV-Vis absorption spectrum of compound 3

Figure 7 shows the UV-Vis absorption of compound 3 and the absorption wavelength maximum is at about 495nm. The energy gap (Eg) of the highest occupied molecular orbital (HOMO) and lowest unoccupied molecular orbital (LUMO) could be calculated approximately based on the UV-Vis absorption of compound 3 by using the Equation (1):

$$Eg\ (eV) = hc/\lambda = 1240/\lambda\ (\lambda: nm) \qquad \text{Eq. 1}$$

Where h is Planck constant (4.135×10^{-15} eV s), c is the speed of light (3.0×10^{17} nm/s), hc = 1240 eV nm. λ is the absorption maximum (nm) extracted from the UV-Vis absorption spectrum of the compound[37], and according to Figure 5, λ = 495 nm. Hence, the corresponding energy gaps, Eg, for compound 3 can be calculated as 2.50 eV, which shows a relatively low energy gap. The electron density distribution of the HOMO and LUMO states calculated by TD-DFT using Gaussian 16 at the B3PW91/6–31G(d) level was also shown in Figure 8 and the electron cloud is mainly localised on the conjugated perylene core. The result shows the optical absorption wavelength and energy gap is mainly determined by conjugated aromatic structures.

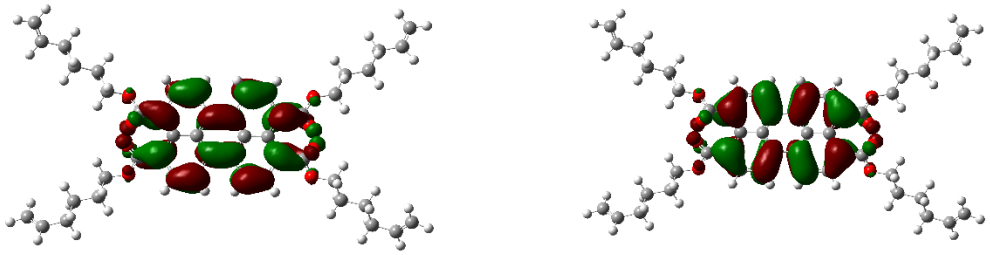

(a) HOMO of compound 3 (b) LUMO of compound 3

Figure 8. The HOMO and LUMO states of compound 3 by TD-DFT calculation using Gaussian 16 at the B3PW91/6–31G(d) level.

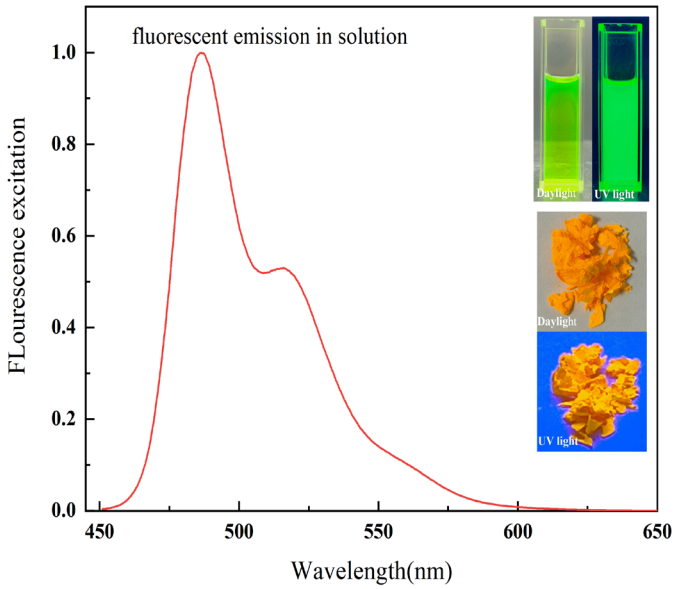

Figure 9. Normalised spectrum of fluorescence emission for compound 3 in solution and its colours in solution and in powder under daylight and UV light.

The fluorescent emission spectrum of compound 3 was also measured to further study its luminescent properties. Figure 9 gives fluorescent emission spectrum of compound 3 and its colours in solution and in powder under daylight and UV light. It can be seen clearly that compound 3 in dichloromethane exhibits yellowish green colour under daylight and green fluorescence under 365 nm UV light, while the powder shows orange-yellow colour under daylight and fluorescent yellow under 365 nm UV light. This shows that there is a blue shift when compound 3 was dissolved in solvent, and the bright colours observed suggest that the perylene-based liquid crystalline compound 3 is a good candidate for fluorescent materials.

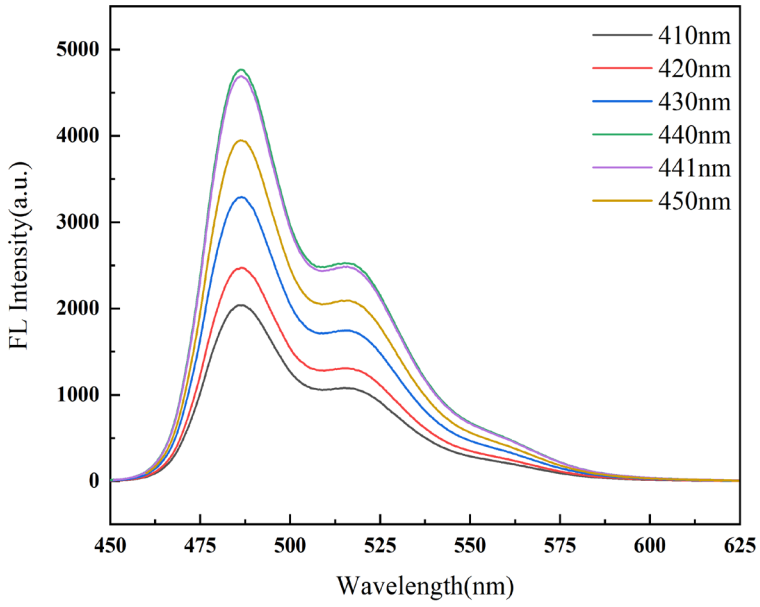

Figure 10. The Fluorescence emission spectra of compound 3 in different excited states.

In addition, the fluorescence emission spectra of compound 3 in different excited states were compared in Figure 10. The fluorescence intensity showed a trend of increasing and then decreasing as the excitation wavelength increased from 410 nm to 450 nm in 10 nm increments, and the highest fluorescence intensity is observed at 440 nm. The fluorescence patterns show no obvious shift in the peak position of the fluorescence emission when the excitation wavelength is increased. This indicates that the characteristics of the fluorescence emission spectra are not affected by the excitation wavelength, and are reflecting the intrinsic electronic structure and energy levels of the fluorescent material.

Conclusion

In summary, a novel polymerisable perylene-tetra(carboxylate-hexene) liquid crystal was successfully synthesized via a straightforward one-step route. Its mesomorphic behaviour and transition temperatures were fully investigated using POM, DSC and SAXS/WAXS. The combined experimental results suggest that this disc-like molecule does not form a common hexagonal columnar mesophase. Instead, it self-assembles into a layer-like (lamellar) structure due to the decreased length of the four peripheral hexene chains. The optimised 3D geometry model confirms the classic disc-shaped configuration of the single molecule. This model was pivotal in building a structure-property relationship, highlighting that while the intrinsic molecular shape is discotic, the shortened chains dictate a collective lamellar packing in the bulk state. Furthermore, the compound with a relatively low energy gap of approximately 2.5 eV exhibits yellowish green colour under daylight and green fluorescence under UV light (365 nm), while its powder shows orange-yellow colour under daylight and fluorescent yellow. The luminescent liquid crystal with a room-temperature, wide range of mesophase, establish this material as a promising candidate for application as a fluorescent organic semiconductor.

Conflict of Interests

The authors declare no conflict of interests.

Funding

Authors acknowledge the financial support from the National Natural Science Foundation of China (62204093 and 22205155), International Exchanges 2023 Cost Share from the Royal Society (IEC\NSFC\233501), the Young Elite Scientists Sponsorship Program by Jiangsu Association for Science and Technology (JSTJ-2023-XH042).

ORCID

Guang Hu, http://orcid.org/0000-0003-4883-0866
Huanjun Lu, http://orcid.org/0000-0003-1666-6731

References

[1] D. Becker *et al.*, ACS Appl. Electron. Mater. 6 (2), 1234 (2024).

doi:10.1021/acsaelm.3c01586
[2] E. Aksoy *et al.*, Dyes Pigments. 211, 111050 (2023). doi:10.1016/j.dyepig.2022.111050
[3] D. Li *et al.*, Adv. Funct. Mater. 33 (45), 2305012 (2023). doi:10.1002/adfm.202305012
[4] Q. Jiang *et al.*, Adv. Mater. 34 (14), 2108103 (2022). doi:10.1002/adma.202108103
[5] S. Kumagai *et al.*, Acc. Chem. Res. 55 (5), 660 (2022). doi:10.1021/acs.accounts.1c00548
[6] S. Wirsing *et al.*, J. Phys. Chem. C. 123 (45), 27561 (2019). doi:10.1021/acs.jpcc.9b07511
[7] S. Rani *et al.*, J. Mol. Liq. 385, 122202 (2023). doi:10.1016/j.molliq.2023.122202
[8] P. K. Behera *et al.*, Chem. Euro. J. 30 (23), e202304333 (2024). doi:10.1002/chem.202304333
[9] V. K. Vishwakarma *et al.*, ACS Appl. Electron. Mater. 5 (4), 2351 (2023). doi:10.1021/acsaelm.3c00179
[10] R. K. Gupta *et al.*, Langmuir 35 (7), 2455 (2018). doi:10.1021/acs.langmuir.8b01081
[11] A. L. Alves *et al.*, Beilstein J. Org. Chem. 19 (1), 1755 (2023). doi:10.3762/bjoc.19.128
[12] P. K. Behera *et al.*, Chem. Asian J. 18 (9), e202300086 (2023). doi:10.1002/asia.202300086
[13] S. Chen *et al.*, Liq. Cryst. 45 (6), 793 (2018). doi:10.1080/02678292.2017.1383522
[14] T. M. Swager, Acc. Chem. Res. 55 (20), 3010 (2022). doi:10.1021/acs.accounts.2c00452
[15] L. B. Avila *et al.*, J. Mol. Liq. 402, 124757 (2024). doi:10.1016/j.molliq.2024.124757
[16] G. Hu *et al.*, Liq. Cryst. 48 (5), 626 (2021). doi:10.1080/02678292.2020.1800847
[17] P. K. Behera *et al.*, J. Mater. Chem. C. 12 (19), 6893 (2024). doi:10.1039/D3TC04407F
[18] J. De *et al.*, ACS Appl. Mater. Interfaces. 11 (8), 8291 (2019). doi:10.1021/acsami.8b18749
[19] S. Dhingra *et al.*, J. Mol. Liq. 390, 122984 (2023). doi:10.1016/j.molliq.2023.122984
[20] I. Bala *et al.*, J. Mater. Chem. C. 8 (36), 12485 (2020). doi:10.1039/D0TC02754E
[21] Z. Ma *et al.*, J. Mater. Chem. A. 10, 18542 (2022). doi: 10.1039/D2TA05358F
[22] V. C. Wakchaure *et al.*, Angew. Chem. Int. Edit. 62 (34), e202307381 (2023). doi:10.1002/anie.202307381
[23] R. Duan *et al.*, J. Mater. Chem. C. 12, 6671 (2024) doi:10.1039/D4TC00295D
[24] W. Zhao *et al.*, Prog. Polym. Sci. 114, 101365 (2021). doi:10.1016/j.progpolymsci.2021.101365
[25] M. Mizusaki, Mol. Cryst. Liq. Cryst. 768 (4), 76 (2024). doi:10.1080/15421406.2023.2274664
[26] G. Hu *et al.*, Addit. Manuf. 55, 102861 (2022). doi:10.1016/j.addma.2022.102861

[27] Y. Wang *et al.*, Adv. Funct. Mater. 33 (4), 2210614 (2022). doi:10.1002/adfm.202210614
[28] M. Barnes *et al.*, ACS Appl. Mater. Interfaces. 12 (25), 28692 (2020). doi:10.1021/acsami.0c07331
[29] M. Chen *et al.*, Adv. Mater. 35 (23), 2209566 (2023). doi:10.1002/adma.202209566
[30] B. Du *et al.*, J. Polym. Sci. 2024. doi:10.1002/pol.20240084
[31] F. Ge *et al.*, Adv. Funct. Mater. 30 (2), 1901890 (2020). doi:10.1002/adfm.201901890
[32] R. K. Gupta *et al.*, Langmuir 31, 8092 (2015).doi:10.1021/acs.langmuir.5b01187
[33] F. Zander *et al.*, Macromol. Chem. Phys. 211, 1167 (2010). doi:10.1002/macp.200900659
[34] C. Tschierske, J. Mater. Chem. 11(11), 2647 (2001). doi:10.1039/B102914M
[35] C. Tschierske, Curr. Opin. Colloid Interface Sci. 7(1-2), 69 (2002). doi:10.1016/S1359-0294(02)00014-6
[36] W. Hu *et al.*, Phase Transit. 98(2-3), 215 (2025). doi:10.1080/01411594.2025.2481139
[37] G. Hu *et al.*, Mol. Cryst. Liq. Cryst. 723 (1), 80 (2021). doi:10.1080/15421406.2021.1895960